DOI: 10.1534/genetics.104.035691

A Genetic Screen for Suppressors of Drosophila NSF2 Neuromuscular Junction Overgrowth

Matthew J. Laviolette,* Paula Nunes,* Jean-Baptiste Peyre,† Toshiro Aigaki† and Bryan A. Stewart*,[1]

†*Department of Biology, Tokyo Metropolitan University, Tokyo 192-0397, Japan and*
**Department of Life Sciences and Zoology, University of Toronto at Scarborough, Toronto, Ontario M1C 1A4, Canada*

Manuscript received September 8, 2004
Accepted for publication March 15, 2005

ABSTRACT

The Drosophila larval neuromuscular system serves as a valuable model for studying the genes required for synaptic development and function. *N*-Ethylmaleimide sensitive factor (NSF) is a molecule known to be important in vesicular trafficking but neural expression of a dominant negative form of NSF2 induces an unexpected overgrowth of the Drosophila larval neuromuscular synapse. We have taken a genetic approach to understanding this novel phenotype by conducting a gain-of-function modifier screen to isolate genes that interact with the overgrowth phenotype. Our approach was to directly visualize the neuromuscular junction (NMJ) using a GFP transgene and screen for suppressors of NMJ overgrowth using the Gene Search collection of *P*-element insertions. Of the 3000 lines screened, we identified 99 lines that can partially restore the normal phenotype. Analysis of the GS element insertion sites by inverse PCR and comparison of the flanking DNA sequence to the Drosophila genome sequence revealed nearby genes for all but 10 of the 99 lines. The recovered genes, both known and predicted, include transcription factors, cytoskeletal elements, components of the ubiquitin pathway, and several signaling molecules. This collection of genes that suppress the NSF2 neuromuscular junction overgrowth phenotype is a valuable resource in our efforts to further understand the role of NSF at the synapse.

FIRST identified for its role in vesicle transport within the Golgi apparatus (Block *et al.* 1988), *N*-ethylmaleimide sensitive factor (NSF) has been shown to be important for vesicular trafficking between many cellular compartments in a variety of cell types. Molecular and biochemical studies (Whiteheart *et al.* 1992, 1994; Sollner *et al.* 1993a,b) have demonstrated that NSF is an ATPase which, through the adaptor protein α-SNAP (soluble NSF attachment protein), can bind a protein complex of SNAP receptors (the SNARE complex). The SNARE complex is a tripartite complex (Sollner *et al.* 1993b) consisting of VAMP, syntaxin, and SNAP-25. A *trans*-membrane SNARE complex consisting of VAMP on the vesicle and syntaxin and SNAP-25 on the target membrane is thought to form the core molecular machinery that can mediate vesicular fusion (Weber *et al.* 1998; Parlati *et al.* 1999). Following fusion and incorporation of the vesicle into the target membrane, all three members of the SNARE complex reside in the same membrane: this is called a *cis*-SNARE complex. NSF and α-SNAP can bind the *cis*-SNARE complex and upon ATP hydrolysis the barrel-shaped NSF hexamer rotates and imparts torsional force on the SNARE complex through α-SNAP. This force disassembles the SNARE complex, freeing the individual SNAREs for further rounds of vesicle fusion.

In addition to this canonical role for NSF, other roles have recently emerged (Whiteheart and Matveeva 2004). The most widely studied new role for NSF is in trafficking of postsynaptic α-amino-3-hydroxy-5-methylisoxazole-4-propionic acid (AMPA)-type glutamate neurotransmitter receptors (Nishimune *et al.* 1998; Song *et al.* 1998). Insertion and retrieval of neurotransmitter receptors is thought to be an important mechanism regulating synaptic strength (Nishimune *et al.* 1998; Noel *et al.* 1999) and NSF is an important molecule regulating receptor trafficking. It appears that the ATPase activity of NSF is important for regulating the disassembly of a protein complex containing a glutamate receptor subunit (GluR2) and PICK-1 (Hanley *et al.* 2002). These data show that non-SNARE protein complexes can act as substrates for NSF's activity and raise the possibility that NSF interacts with non-SNARE proteins in the presynaptic nerve terminal as well.

Other recently identified molecules that interact with NSF include G-protein-coupled receptors, Lma1, GATE-16, and rab6 (Xu *et al.* 1998; McDonald *et al.* 1999; Han *et al.* 2000; Cong *et al.* 2001; Muller *et al.* 2002). Altogether these interactions indicate that NSF likely has a large repertoire of cellular functions.

[1]*Corresponding author:* Department of Life Sciences, University of Toronto at Scarborough, 1265 Military Trail, Toronto, ON M1C 1A4, Canada. E-mail: stewart@utsc.utoronto.ca

Drosophila has two NSF isoforms that share 80% amino acid identity (Boulianne and Trimble 1995; Pallanck *et al.* 1995) and they can functionally substitute for each other (Golby *et al.* 2001). NSF1 is the functionally predominant isoform in the adult central nervous system, while NSF2 is functional throughout early development in neural and nonneural tissue. Null alleles of NSF1 die as pharate adults while NSF2 null alleles die early as first instar larvae (Golby *et al.* 2001). We wished to study synaptic development and function at the accessible larval neuromuscular synapse. To circumvent the lethality associated with severe NSF2 mutants, we generated dominant-negative NSF2 constructs (*NSF2$^{E/Q}$*; Stewart *et al.* 2001) that can be expressed in a tissue-specific manner, in the wild-type background. When expressed in larval neurons, this *NSF2$^{E/Q}$* construct suppresses synaptic transmission, reduces the size of the pool of releasable synaptic vesicles, and increases synaptic fatigue (Stewart *et al.* 2002). Surprisingly, we also observed a dramatic overgrowth of the neuromuscular junction. This phenotype is not likely a response to impaired synaptic physiology since mutations in *syntaxin* or *n-synaptobrevin* that reduce synaptic transmission to comparable levels do not have a hypersprouting phenotype at the neuromuscular junction (NMJ) (Stewart *et al.* 2000). Thus, in contrast to the other SNARE mutants, it appears that the overgrowth phenotype is unique to NSF and may indicate that NSF additionally plays a developmental role at the NMJ. To further understand the overgrowth phenotype, and to identify genes that interact with NSF, we have conducted a suppressor screen to identify genes that, when overexpressed, can restore the NSF2 mutant NMJ morphology to normal.

MATERIALS AND METHODS

Drosophila stocks and genetics: All crosses were carried out at 25° and stocks were maintained on Bloomington standard medium (http://flystocks.bio.indiana.edu/bloom-food.htm). We carried out an overexpression/misexpression screen using a Gene Search (GS) collection of *P*-element insertions that drive the expression of nearby genes under control of the yeast transcriptional activator Gal4 (Toba *et al.* 1999). The special feature of this collection is that the *P* elements bear Gal4 upstream activation sequence (UAS) at both ends of the transposon and therefore they can potentially drive gene expression in two directions. The GS elements improve the efficiency of misexpression screening ~10-fold compared to enhancer promoter (EP) elements, which drive gene expression in one direction only (Toba *et al.* 1999). In addition, we screened unidirectional misexpression lines carrying P{GS2}, P{GS3}, and P{GS6} vectors (T. Aigaki, unpublished results; see http://www.comp.metro-u.ac.jp/%7Eatsugyou/gs/Methods/Vectors/GSvectors.html).

Generation of dominant-negative *UAS-NSF2$^{E/Q}$* is described in Stewart *et al.* (2001), and the recombinant third chromosome bearing *elav^{3A}-Gal4* and *UAS-NSF2$^{E/Q}$* is described in Stewart *et al.* (2002). *P{Mhc.CD8-GFP-Sh}*, described in Zito *et al.* (1999), carries the myosin heavy chain (MHC) promoter driving the expression of a chimeric GFP fusion protein bearing the CD8 transmembrane domain and the C-terminal of the Shaker potassium channel. This fusion protein concentrates at type I neuromuscular junction boutons, thus providing postsynaptic GFP labeling of the NMJ.

Screening for NMJ overgrowth suppressors: We directly screened for changes in NMJ morphology using the GFP transgene as first described in Parnas *et al.* (2001). A total of 5–10 virgin females of the stock *w Mhc.CD8-GFP-Sh; elav^{3A}-Gal4.UAS-NSF2$^{E/Q}$/TM6B,Tb* were mated to three to five males from viable gene search lines. Non-*Tb* larval offspring were selected for direct analysis of NMJ morphology. For GS lines that were known to be located on the X chromosome, the sexes were reversed and only female non-*Tb* larvae were examined. In total, ~3000 GS lines were screened. To visualize the NMJ in the intact larvae, we immobilized the larvae by placing up to four of them in a 0.2-ml tube with 100 μl of glycerol that was heated to 60° for 10 sec in a thermocycler. The larvae were then placed onto glass slides in glycerol with a coverslip, which was used to role the larvae into a lateral orientation.

GFP signals were viewed at the neuromuscular junction within the intact larvae on a Nikon E600FN microscope using a ×40 long working distance objective. Fluorescent illumination was provided by a 100-W Hg bulb and GFP filter set. A Hammamatsu ORCA ER camera was used to visualize the GFP signals, and images of NMJs from intact larvae were acquired with SimplePCI software (Compix, Mars, PA).

We routinely scored NMJs of muscles 12 and 13 since they have a reasonably unobstructed view in the intact larva and they could be easily identified by first locating the lateral end of the denticle belts and then identifying the triangle formed by muscles 12, 5, and 8. Occasionally we scored NMJs of muscles 6/7 or muscle 4, but these were usually harder to visualize in the intact animal.

Immunocytochemistry: For tertiary screening to confirm the observations made in the intact larvae, we dissected third instar larvae in HL3 saline (Stewart *et al.* 1994), fixed the preparation in 4% formaldehyde for 10 min, washed the preparation in phosphate-buffered saline plus 0.1% Triton X-100 for 30 min, followed by a 1- to 2-hr incubation at room temperature, or overnight at 4°, in 1:1000 dilution of FITC-conjugated goat anti-HRP antibody (ICN Biochemicals). The preparations were washed for another 30 min and then mounted in Vectashield (Vector Labs, Burlingame, CA) for microscopic analysis. Neuromuscular junction rescue data were tabulated using Microsoft Access and analyzed using Microsoft Excel and Graphpad Prism 3.0. Images were acquired on a Zeiss LSM 510 confocal microscope with a ×40 oil immersion lens by collecting z-sections at 1-μm intervals and projecting the images onto a single plane.

Identification of P{GS} insertion sites: Standard molecular methods for inverse polymerase chain reaction (PCR) were used to identify the insertion sites of the GS elements. In brief, DNA was prepared from ~30 adult flies and digested with *Sau*3AI or *Msp*I (for 5′ sequence of GS lines 5000–5999 and 7000–7999). The DNA fragments were then ligated overnight at 4° with T4 DNA ligase. Ligated fragments were next amplified via PCR with primer sets designed to amplify from P{GS}sequence. Detailed methods, including primer sequences, are available at http://www.comp.metro-u.ac.jp/%7Eatsugyou/gs/Methods/protocol.html.

Following amplification, the PCR products were analyzed by DNA sequencing using the following sequencing primers: 5′seq, TCGTCCGCACACAACCTTTC; 3′pseq, CTCACTCA GACTCAATACGAC. The DNA sequence data flanking the GS element insertions were compared to the Drosophila genome sequence, made publicly available by the Berkeley *Drosophila* Genome Project, and the GS elements were thus superimposed on the genomic map of known and predicted genes.

Quantitative RT-PCR for GS vector flanking genes: GS lines were crossed to hs-GAL4 stock (P{GAL4-Hsp70.PB}89-2-1). The resulting third instar larvae were heat induced for 45 min at 37°, allowed to recover for 1 hr at 25°, and then homogenized in QIAGEN (Chatsworth, CA) RLT buffer using FASTPREP FP120 (BIO101) with lysing matrix D (BIO101). Lysate was eluted through a Qiashredder, and total RNA was then isolated using a QIAGEN RNeasy mini kit. Fifty micrograms of total RNA was treated with RNase free DNase I (TAKARA) to eliminate genomic DNA contamination. Two micrograms of total RNA was used as template for reverse transcription (Invitrogen SuperScript III RNase H free reverse transcriptase), and the resulting cDNA samples were then used as templates for quantitative PCR using PTC-200 cycler equipped with a Chromo4 real-time fluorescence detector (MJ Research, Watertown, MA). PCR was carried out with TAKARA SYBR Premix Ex Taq and a pair of gene-specific primers (listed below). RpL32 ribosomal protein mRNA in each sample was also quantified as an internal control using primers RP49-F2 GCTAAGC TGTCGCACAAATG) and RP49-R TGTGCACCAGGAACTTC TTG). We used the following amplification parameters: hot start 95° 1 min, then 45 cycles of (95° for 5 sec 57° for 20 sec, 72° for 15 sec). The amount of PCR product was monitored and quantitated using Opticon software (MJ Research). To compare with the endogenous level of mRNA, samples were prepared from the corresponding GS lines and subjected to quantitative PCR. Experiments were repeated four times for each genotype.

The following forward (f) and reverse (r) gene-specific primers were used: *CG3793(f)* GAAGGACGACTACATCGGGTACTT; *CG3793(r)* GCACTCGGCGAGAAATATGGTGGG; *Gli(f)* CGGC GAATACACGTTCAAGTAGAG; *Gli(r)* TGAAGTCCATCGACA TCTACACGG; *Snap(f)* GATGGTGGTGTACCACTGATCCAA; *Snap(r)* GATGGTGGTGTACCACTGATCCAA; *polo(f)* AAGC ATTACGGAGTTCGAATGCCG; *polo(r)* AAGAACATGGGCAC CTTTGAGCCC; *CG32225(f)* CTGCCTCAACGTGGCACTGA TTTA; and *CG32225(r)* CCTTGTCGCAGACATAGGACTTAC.

RESULTS AND DISCUSSION

Screening for NMJ suppressors: To search for suppressors of the $NSF2^{E/Q}$ hypersprouting phenotype, we used flies that carry a GFP fusion that contains a CD8 transmembrane domain and the Shaker K+ channel C terminus driven directly in muscle by the MHC promoter. GFP expressed by this construct is localized on the postsynaptic side of the NMJ and faithfully reports NMJ structure (Zito *et al.* 1997). These flies also contained a recombinant third chromosome that has $elav^{3A}$-*GAL4* and $UAS\text{-}NSF2^{E/Q}$ and we crossed the line to the GS library to obtain offspring with $UAS\text{-}NSF2^{E/Q}$ and the GS element driven in neurons by *elav-GAL4*. To assay NMJ morphology directly, we visualized GFP signals through the larval cuticle and examined NMJs in larvae coexpressing $UAS\text{-}NSF2^{E/Q}$ and one of the GS lines. We selected lines that appeared more normal than $UAS\text{-}NSF2^{E/Q}$ alone. Control *UAS-GFP* transgenes failed to suppress the overgrowth, indicating that dilution of GAL4 transcription factor by the additional binding sites is not responsible for the GS lines identified.

The $NSF2^{E/Q}$ hypersprouting phenotype is extremely penetrant, showing clear defects in every hemi-segment of the larval bodywall. The hallmarks of this mutant allele are very long nerve terminal branches, supernumerary branches, and small synaptic boutons. Thus, it is relatively easy to score rescue of this phenotype since any change toward normal is an indicator of genetic interaction. We concentrated our screen of intact NMJs on muscles 12 and 13 and used two criteria to judge rescue, reduction of nerve terminal branch length, and restoration of synaptic bouton morphology (Figure 1). For our initial screen, we categorized rescued animals into strong, moderate, and weak rescues with the strong categorization reserved for lines that produced nearly normal NMJs in several hemi-segments. The moderate and weak descriptors were used for those lines that showed some degree of rescue of either branch length or bouton number in a fewer number of hemi-segments. We scored at least three intact larvae per GS line and kept lines in which weak rescue was observed in at least two hemisegments. From the initial screen we kept ~300

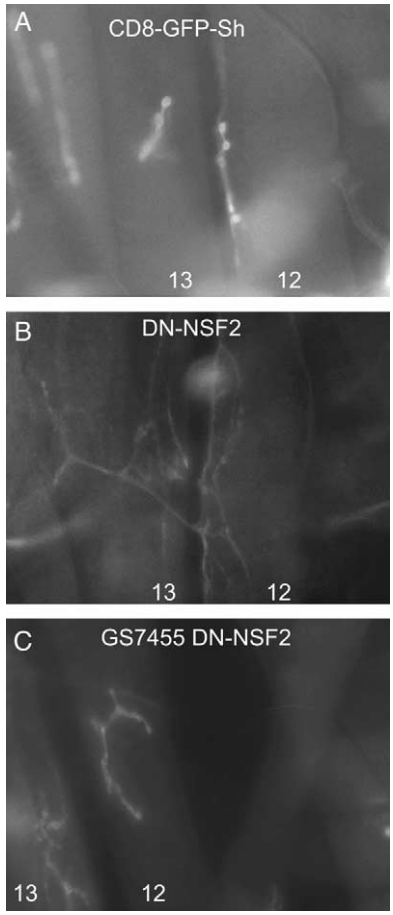

Figure 1.—Intact neuromuscular junctions. These images were obtained by visualization of CD8-GFP-Sh through the cuticle of intact larvae and represent exactly the images we used to score suppressors in our screen. All images are from muscles 12 and 13. (A) CD8-GFP-Sh expressed in a wild-type background. (B) A typical *elav-Gal4*: $UAS\text{-}NSF2^{E/Q}$ neuromuscular junction in which the GFP signal is less intense due to the hypersprouting phenotype. (C) A suppressor result from GS7455, in which the muscle 12 NMJ is substantially restored.

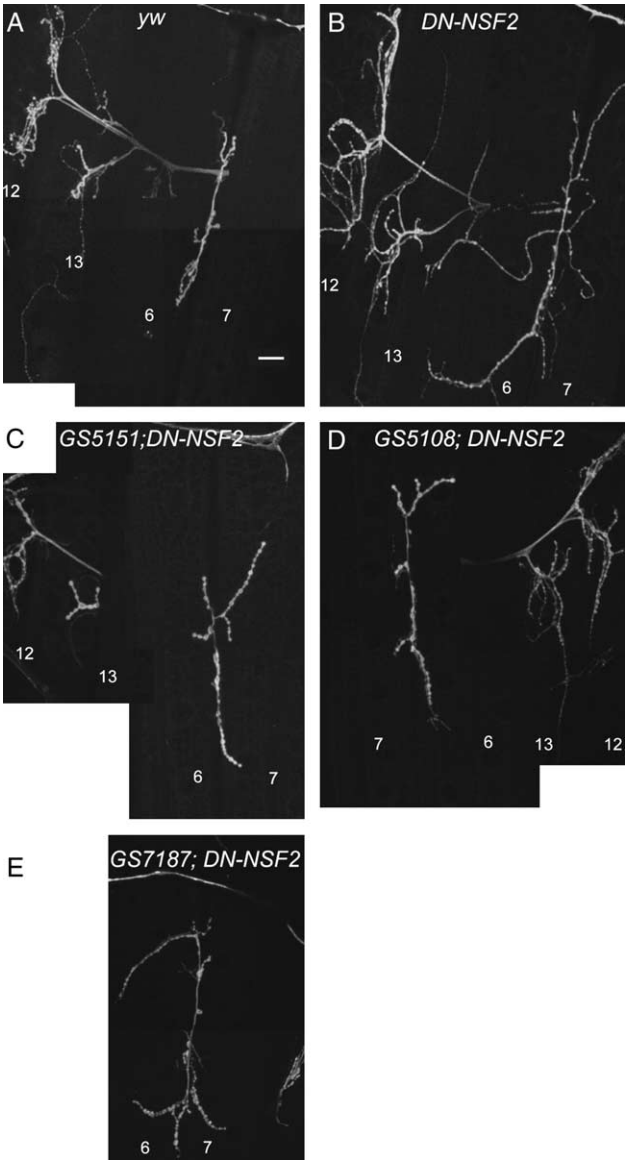

Figure 2.—Immunohistochemistry of suppressor lines. These images were obtained by dissecting larvae of the indicated genotypes and labeling their NMJs with FITC anti-HRP. (A) Typical muscle 6, 7, 12, and 13 NMJs from *yw* control larvae. (B) Example of a typical *UAS-NSF2*$^{E/Q}$ larval preparation in which the NMJs are very overgrow and show very long and supernumerary branches. (C) Example of a strong rescue from GS5151 in which all of the NMJs of muscles 6/7, 12, and 13 were rescued in this hemi-segment. (D) A more typical example from GS5108 in which the muscle 6/7 NMJ shows recovery but muscles 12 and 13 continue to display a mutant phenotype. This hemi-segment would be scored "strong rescue" on muscle 6/7 and "no rescue" on muscle 12/13. (E) An example of a muscle 6/7 NMJ from GS7187 that shows substantial recovery of bouton morphology but some long branches remain. Bar, 25 μm for A–E.

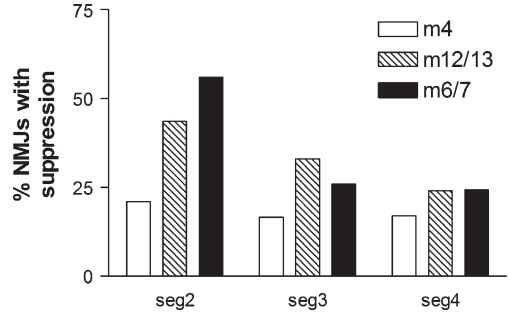

Figure 3.—Muscle- and segment-specific pattern of suppression. We analyzed the degree of suppression for muscles 6/7, 12/13, and 4 in abdominal hemi-segments 2, 3, and 4. The bar graph shows the percentage of NMJs that were scored as suppressors. On average, more NMJs were scored with suppression in segment 2 than in the other segments.

lines. We next rescreened these GS lines and retested the ability of the GS lines to rescue the phenotype. After the second round of scoring we kept 99 GS lines from the 3000 initially screened for further analysis.

Strength and penetrance of suppression: To confirm our observations, we dissected 4–6 larvae from 74 of the lines for conventional immunocytochemical analysis of NMJ morphology of muscles 6 and 7, 12 and 13, and 4 in each of abdominal segments 2, 3, and 4 (Figure 2). Accordingly, of the 2358 NMJs examined, we scored rescue in each of the 74 lines and of the 393 larvae analyzed, only 7 larvae, each from a different GS line, failed to show appreciable rescue. Therefore, since we observed rescue in 100% of the 74 GS lines and in 98.2% of the larvae examined, we are confident that each of the 97 GS lines that emerged from our rescreening are genuine genetic suppressors of the NSF2 overgrowth phenotype.

In our fluorescence microscopy examination of 74 GS lines, we scored each NMJ as showing strong, moderate, or no rescue. From this data we found that 255 of the 393 larvae, from 71 different GS lines, showed at least one NMJ with strong rescue. Examples of the NMJs are shown in Figure 2. We further analyzed the degree of rescue in different abdominal segments and in different muscles (Figure 3). The most noteworthy observation is the larger degree of rescue observed in m6/7 and m12/13 in segment 2, compared to the other segments. Nearly 50% of m6/7 NMJs and m12/13 NMJs examined showed either moderate or strong rescue in segment 2, whereas in segments 3 and 4, ~25% of the NMJs showed some degree of rescue. The muscle 4 NMJ shows rescue in ~25% of NMJs in all the segments examined. Therefore, we conservatively expect to observe rescue in ~1/4 of m6/7 or m12/13 NMJs in the GS lines examined.

Finally, we documented the degree of rescue associated with each of the 74 GS lines examined. The distribution of the mean number of NMJs showing strong rescue and the distribution showing strong plus moderate rescue (*i.e.*, total) is shown in Figure 4. Of the 18 NMJs examined per animal, the mean number of NMJs showing a strong rescue was 1.4/larvae. Six of the GS lines had mean values of 3 strongly rescued NMJs per larvae or more: 1195, 2091, 2264, 5108, 5151, and 11180. When we examined the number of NMJs showing mod-

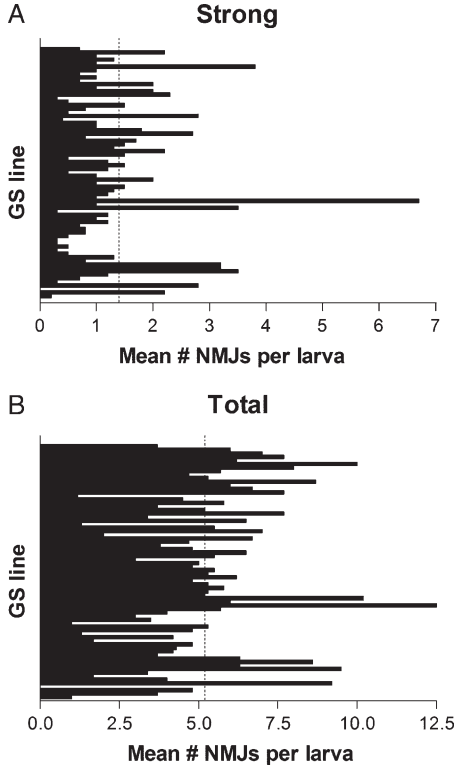

Figure 4.—Strength and penetrance of rescue. We categorized the 2358 NMJs from 74 GS lines as having "no rescue," "weak rescue," or "strong rescue" from our immunohistochemical studies. (A) The mean number of NMJs per larvae (maximum is 18) that were judged as showing strong rescue for each of the GS lines. The mean number of strongly rescued NMJs per larvae was 1.3, indicated by the dotted line. (B) The mean number of NMJs per larvae showing strong or weak rescue; the mean value, indicated by the dotted line, is 5.1. Individual GS numbers are not shown on the vertical axis.

erate or strong rescue, we found that the mean number of NMJs per larvae showing some degree of rescue is 5.3 NMJs/larvae.

Identification of genes: As part of the Drosophila Gene Search Project (T. Aigaki, unpublished results) we mapped the P{GS}element insertions by inverse PCR and identified the GS element insertion site by BLAST sequence analysis of flanking DNA. The insertion sites were superimposed upon the Drosophila genomic sequence and nearby genes were identified. The candidate genes associated with the GS insertions are listed in Table 1. For 10 of the 99 lines—32, 1027, 2192, 2285, 3087, 5036, 5071, 14410, 14471, and 14505—we were not able to obtain unambiguous flanking sequence information. For the remaining 89 genes, we used the Computed Gene (CG) numbers to batch download the Gene Ontology terms assigned to the genes from FlyBase (http://flybase.bio.indiana.edu/). Many of genes segregate into distinct categories.

Regulators of gene expression: We found 18 GS lines whose candidate genes can be broadly categorized as transcriptional regulators. Several of these candidate genes are known from previous studies to be expressed in the nervous system or in some cases loss-of-function alleles are known to produce neural phenotypes. These are *longitudinals lacking*, *buttonless*, *couch potato*, *hoi polloi*, *E2f*, *brain tumor*, *nejire*, and *retinoblastoma-family protein*.

Interestingly, Marek *et al.* (2000) have examined cyclic AMP response element-binding protein (CREB) (*nejire*) function at larval neuromuscular synapses and while they found that the presynaptic overexpression of CREB impaired neurotransmitter release, it had no effect on presynaptic morphology. Here we found that a GS line in position to overexpress CREB in the $NSF2^{E/Q}$ mutant background rescues the overgrowth phenotype, suggesting that this gene may have a role in presynaptic development.

Three of the 18 transcriptional regulators, *buttonless*, *couch potato*, and *hoi polloi*, were previously recovered in loss-of-function screens designed to uncover genes important for peripheral nervous system development (Salzberg *et al.* 1997; Prokopenko *et al.* 2000). Our results indicate the potential for these genes to also be involved in motor neuron development.

One gene that we recovered, *ovo*, is not normally associated with neural function. *ovo* is normally expressed in the male and female germline cells, where it controls F-actin extension. When expressed in the eye under UAS/Gal4 control, eye bristle formation is impaired and induces ectopic extensions from the ommatadia (Delon *et al.* 2003), suggesting that it has a strong influence on cytoskeletal remodeling (see *Cytoskeletal components and regulators* below).

Currently no expression data or mutational analysis is available for *skuld*, *His2av*, *CG10865*, *CG4119*, *CG6388*, and *CG31782* so it is difficult to determine whether the effects we see here are gain-of-function overexpression effects or the effect of misexpression.

Cytoskeletal components and regulators: It is likely that overgrowth of the neuromuscular junction ultimately affects the underlying cytoskeleton but it was somewhat surprising to identify a large number of genes composing structural components of the cytoskeleton or enzymes with the potential to regulate cytoskeletal dynamics. The structural genes are *Actin5c*, *moesin*, *fimbrin*, *syntrophin-like 2*, *Myosin binding subunit*, *Ptpmeg*, and *CG5740*. Two genes that encode proteins with enzymatic activity that have the potential to regulate the cytoskeleton, *RhoBTB* and *RhoGap18B*, were also found.

Actin5C is one of two cytoplasmic actins in Drosophila and it is highly expressed in many tissues throughout development (Fyrberg *et al.* 1983). It has been studied extensively in many processes, including spermatogenesis and dorsal closure (Kiehart *et al.* 2000; Noguchi and Miller 2003). In the nervous system, *Act5c* has been recovered in a screen for changes in bristle number—presumably a reporter of peripheral nervous system development (Norga *et al.* 2003)—and its role has been studied in glial cell function (Sepp and Auld 2003).

TABLE 1

GS lines and associated genes that suppress *NSF2*$^{E/Q}$-induced NMJ overgrowth

GS line	Nucleotide map position	Interaction strength	CG no.	Symbol	Potential antisense	Gene ontology molecular function
1	2745701	Strong	CG9894			
31	4804786	Strong	CG6824	ovo		RNA polymerase II transcription factor activity
51	20294306	Moderate	CG5517	Ide		Zinc ion binding
			CG5701	RhoBTB		Rho small monomeric GTPase activity
1029	14480383	Moderate	CG10521	NetB		Structural molecule activity
1097	6019742	Strong	CG32744			
1103	17022706	Weak	CG8649	Fim		Actin binding structural constituent of cytoskeleton
1122	893055	Moderate	CG14628			
1124	20329882	Moderate	CG1829	Cyp6v1		Electron transporter activity
1166	19618082	Strong	CG11937	amn		Neuropeptide hormone activity
			CG32529[a]			
1188	9426052	Strong	CG12653	btd		RNA polymerase II transcription factor activity
		Strong	CG15319	nej		cAMP response element binding protein binding
1195	13730451	Strong	CG18319	ben	AS	Ubiquitin conjugating enzyme activity
			CG32616	SteDOR		
2046	11616028	Strong	CG4905	Syn2		Cytoskeletal protein binding; structural constituent of cytoskeleton
2091	5602339	Strong	CG12052	lola		RNA polymerase II transcription factor activity; receptor binding; serine esterase activity
2150	15740868	Strong	CG3903	Gli		
			CG3793			
2162	16764031	Moderate	CG17952			Receptor activity; lamin binding
			CG30404			
2264	16678292	Moderate	CG10321			
			CG9856	PTP-ER		Protein tyrosine phosphatase; Ras signal transduction
3052	22682658	Strong	CG5499	His2Av		DNA binding
			CG6386			Protein kinase activity; protein serine/threonine kinase activity
3056	4303407	Strong	CG31369			
3057	15995779	Weak	CG12284	th		Ubiquitin-protein ligase activity
		Weak	CG32156	Mbs		Myosin binding; structural constituent of cytoskeleton
3062	20228577	Weak	CG12306	polo		Protein serine/threonine kinase activity
			CG32225			
3074	18404090	Moderate	CG5264	btn		RNA polymerase II transcription factor activity
3144	16062131	Weak	CG6303	Bruce		Ubiquitin conjugating enzyme activity
			CG12819	sle		
3152	17435232	Weak	CG6376	E2f	AS	RNA polymerase II transcription factor activity
3199	19868027	Weak	CG5991			Phospholipd metabolism
			CG6000			Chaperone activity
			CG5429			Protease inhibitor activity
3223	328669	Moderate	CG1228	Ptpmeg		Cytoskeletal protein binding; structural constituent of cytoskeleton
			CG6936	mth		G-protein-coupled receptor activity
3234	4087415	Moderate	CG14991		AS	
			CG14992	Ack		Nonreceptor tyrosine kinase activity; SH2-domain binding
3243	12279531	Moderate	CG14895	Pak3		Receptor signaling protein serine/threonine kinase activity

(*continued*)

TABLE 1

(Continued)

GS line	Nucleotide map position	Interaction strength	CG no.	Symbol	Potential antisense	Gene ontology molecular function
			CG10405			Trypsin activity; serine-type endopeptidase activity
3250	1650519	Strong	CG10981			
			CG2023			
3301	16783431	Weak	CG5670	Atpalpha		Sodium/potassium-exchanging ATPase activity
			CG31191			
4009	1690648	Moderate	CG3161	Vha1[a]		Hydrogen-exporting ATPase activity
			CG3274			
4012	16610518	Hoderate	CG3971	Baldspot		Component of plasma membrane
			CG13032			
5044	16668573	Weak	CG17161	grp		Protein serine/threonine kinase activity
5051	11080843	Weak	CG6233	Ufd1-like		Ubiquitin-dependent protein catabolism
5108	13721354	Moderate	CG18319	ben		Ubiquitin-conjugating enzyme activity
5109	18544228	Moderate	CG7095			Regulator of G-protein signaling
5151	8873191	Strong	CG12664	ld14		Plasma membrane
5155	24973209	Moderate	CG11897			Multi-drug transporter activity
5156	4613326	Strong	CG1888			
5162	7734927	Moderate	CG8776			Carbon-monoxide oxygenase activity
		Moderate	CG8772	nemy	AS	Glutaminase activity
5164	16610164	Weak	CG3971	Baldspot		Component of plasma membrane
5167	19112620	Weak	CG10685			DNA-directed RNA polymerase activity
5173	558808	Moderate	CG7413	Rbf		DNA binding; transcription regulator activity
5181	13769814	Moderate	CG31243	cpo	AS	RNA binding
5186	19562121	Weak	CG8798			Endopeptidase La activity
5187	9889733	Weak	CG5920	sop		Structural constituent of ribosome
5189	8086858	Moderate	CG7962	CdsA		Phosphatidate cytidylyltransferase activity
5198	19027140	Strong	CG10473		AS	
			CG15173			
			CG10470			
5212	13493258	Strong	CG32652			
			CG11129	Yp3	AS	Phospholipid metabolism
5216	5642065	Moderate	CG5740	Act5C		Structural constituent of cytoskeleton
5233	4625861	Weak	CG8351			ATPase activity, coupled; chaperone activity
5240	14983831	Strong	CG5637	nos	AS	RNA binding
			CG117799			Protein translocase activity
5246	17705460	Moderate	CG30217			
6075	6177590	Weak	CG10236	LanA		Structural molecule activity; cell adhesion
6084	17441098	Moderate	CG32650			Ras GTPase activator
6087	20943738	Strong	CG10585			*trans*-hexaprenyltranstransferase activity
6103	2085888	Moderate	CG3450			
7040	12416560	Strong	CG6388			Nucleic acid binding; tRNA (guanine-N2-)-methyltransferase activity
7145	1801650	Moderate	CG3268	phtf		
7187	17950476	Weak	CG31423			
			CG5740		AS	Component of cytoskeleton
7274	2349854	Strong	CG7245		AS	Structural molecule activity
			CG9967			
7368	3209817	Weak	CG10801			
7378	2704750	Weak	CG3603			Fatty acid biosynthesis
7381	11734628	Moderate	CG1806			
7387	13493401	Strong	CG32652			
			CG11129	Yp3	AS	Phospholipid metabolism
7406	6028443	Weak	CG15897			

(*continued*)

TABLE 1

(Continued)

GS line	Nucleotide map position	Interaction strength	CG no.	Symbol	Potential antisense	Gene ontology molecular function
7412	6850214	Moderate	CG4626	fz4		Wnt-protein binding; Wnt receptor activity
7455	8634439	Strong	CG10701	Moe		Cytoskeletal protein binding; structural constituent of cytoskeleton
7456	5406461	Moderate	CG4119			RNA binding
8030	2357907	Moderate	CG3664	Rab5		Rab small monomeric GTPase activity
8035	19007814	Weak	CG17894	cnc	AS	RNA polymerase II transcription factor activity
			CG4568	fzo	AS	GTPase activity
8036	24141408	Moderate	CG14066	larp		
			CG14065			
8052	11988549	Weak	CG12264			Cysteine desulfhydrase activity
8156	6532982	Strong	CG3126	C3G		Ras guanyl-nucleotide exchange factor activity
8172	223869	Strong	CG2872	rl[a]		MAP kinase activity
9097	18885245	Moderate	CG7481	RhoGAP18B		GTPase activator activity; small GTPase regulatory/interacting protein activity
			CG7502	CG7502		
9123	14557171	Moderate	CG14411			Phosphoprotein phosphatase activity
9124	22048007					Transposable element TE20200
9657	19549889	Moderate	CG10334	spi		Epidermal growth factor receptor ligand
9705	5595651	Weak	CG12052	lola		RNA polymerase II transcription factor activity
10582	16663196	Weak	CG17161	grp		Protein serine/threonine kinase activity
10710	16705617	Moderate	CG17332	VhaSFD[a]		Hydrogen-exporting ATPase activity, phosphorylative mechanism
			CG31782[a]			Transcription regulator activity
11180	19136449	Strong		brat		Transcription regulator activity
11641	10228537	Weak	CG18285	igl		Calmodulin binding
12020	7614185	Moderate	CG7492			
12852	9693135	Moderate	CG4379	Pka-C1		cAMP-dependent protein kinase activity
			CG3949	hoip	AS	RNA binding; structural constituent of ribosome
14006	16663443	Moderate	CG17161	grp		Protein serine/threonine kinase activity
14189	279164	Weak	CG14651			Nonreceptor tyrosine kinase activity; SH2 domain binding
14358	2550834	Strong	CG1624	dpld		Transcription factor
14514	9495759	Moderate	CG4422	Gdi		GDP-dissociation inhibitor

AS indicates that the GS element is inserted near the 3′-end of the gene with the correct orientation to induce antisense transcripts. Interaction strength indicates our assesment on the secondary screen. GS lines 1–4999 carry bidirectional P{GSV1}; lines 5000–5999 and 7000–7999 carry unidirectional P{GSV2}; lines 6000–6999 and 8000–8999 carry unidirectional P{GSV3}); lines >9000 carry unidirectional P{GSV6}.

[a] The GS element is inserted 3′ to the transcriptional start.

Moesin is a member of the ezrin-radixin-moesin (ERM) family of actin-binding proteins that link actin to the plasma membrane. While a neural role for Drosophila moesin has not previously been reported, it does have a role in growth cone motility in other neural systems (Paglini *et al.* 1998) and a recent report demonstrates the role of Drosophila moesin in photoreceptor rhabdomere development (Karagiosis and Ready 2004).

Ubiquitin pathway components: We additionally identified four genes involved in the ubiquitin protein degradation pathway: *bendless*, *Bruce*, *thread*, and *Ufd1-like*. The gene products of *bendless*, *Bruce*, and *thread* (also known as DIAP1) are thought to act as E2 or E3 ubiquitin-conjugating enzymes (Muralidhar and Thomas 1993; Oh *et al.* 1994; Vernooy *et al.* 2002; Wilson *et al.* 2002). The *Ufd1-like* gene encodes a transcript that is involved in ubiquitin-dependent protein degradation (Ratti *et al.* 2001). Thus, the four candidates in this category would all have the potential to enhance ubiquitin-dependent protein degradation if their expression is increased.

Identification of these genes is an important finding in light of previous developmental NMJ studies, which

revealed that loss-of-function mutants of *highwire*, whose gene product contains a RING finger domain implicated in E3 ubiquitin ligase activity, lead to NMJ overgrowth (Wan *et al.* 2000) that is very similar to $NSF2^{E/Q}$-induced overgrowth. Furthermore, transgenic overexpression of *fat facets* also causes excessive NMJ overgrowth (Diantonio *et al.* 2001). *faf* encodes a deubiquitinating protease (Huang *et al.* 1995) and is thought to protect ubiquitinated proteins from degradation.

Therefore, *hiw* loss of function or *faf* overexpression should lead to reduced ubiquitin-dependent protein degradation. Since the $NSF2^{E/Q}$ phenotype is rescued by expression of genes that should increase the ubiquitin degradation pathway, we infer that reduced ubiquitin pathway function may also be one of the molecular dysfunctions underlying the $NSF2^{E/Q}$ phenotype.

Signaling proteins: We identified three genes involved in G-protein-receptor-coupled signaling: *methuseleh* (*mth*), *Frizzled 4*, and *AlstR*. *methuseleh* is a gene first identified for its effects on life span (Lin *et al.* 1998) and prior analysis of *mth* at the NMJ, using hypomorphic loss-of-function mutants, revealed no effect on the number of synaptic boutons or length of NMJ branches (Song *et al.* 2002). Our results suggest that *mth* may have a previously undetected developmental role at the synapse.

Frizzled 4 is a Wnt receptor that is expressed in the CNS (Janson *et al.* 2001) but so far there has been no genetic analysis of this receptor. However, a recent study has demonstrated the involvement of Wnt signaling at the Drosophila NMJ, showing that *wingless* (*wg*) loss of function resulted in fewer boutons while presynaptic *wg* overexpression produced more boutons; these effects are thought to be mediated through the Wnt receptor Frizzled 2 (Packard *et al.* 2002). While it is currently unknown if the CNS expression of *fz4* is presynaptic or not, our result implies that there may be an autocrine component to Wnt signaling at the synapse, as there is during wing development (Hooper 1994).

There is no previous neural expression or mutant data for *Galpha73B*, a component of a trimeric G-protein complex, and it is not presently clear how this gene aids the restoration of $NSF2^{E/Q}$ neuromuscular overgrowth.

Four genes with known or predicted kinase activity were also recovered: *Pka-C1*, *grapes*, *Pak3*, and *CG6386*. Prominent in this group is *Pka-C1*, which encodes cAMP-dependent protein kinase 1. Previous studies of *rutabaga*, the adenylyl cyclase that produces cAMP, and *dunce*, the phosphodiesterase that hydrolyzes cAMP, have shown dramatic effects on NMJ morphology and physiology (Zhong *et al.* 1992). Loss of function of either *rut* or *dnc* leads to NMJ overgrowth, although the extent of that effect is not as large as is seen with the $NSF2^{E/Q}$ allele. Interestingly, GS9123 is inserted 252 bp upstream of the *rutabaga* 5′-UTR; however, the orientation of the UAS sequence appears to be in the wrong direction to drive expression of *rut*.

PAK3 is a member of the p21-activated kinase family that has been shown in other systems to strongly influence the cytoskeleton (Eby *et al.* 1998) by way of its interactions with the small GTPases Rho and cdc42 that directly regulate actin biochemistry. Thus, our finding of PAK3 also potentially fits with our observations of the cytoskeletal components described above.

Three genes with activity in the Ras signaling pathway were found: *C3G, PTP-ER*, and *CG32560*. *C3G* is a RAS family guanine nucleotide exchange factor (Ishimaru *et al.* 1999) that activates Ras by catalyzing exchange of GDP for GTP. *PTP-ER* encodes a tyrosine phosphatase that dephosphorylates Drosophila MAPK (Karim and Rubin 1999), thereby downregulating its kinase activity. *CG32560* is predicted to be a RAS GTPase activator, which would activate GTP hydrolysis and downregulate RAS signaling. Thus, the result of *C3G* appears to be in contradiction to the results of *PTP-ER* and *CG32560*.

The Spitz protein is the EGF receptor (EGFR) ligand that has been implicated in many developmental processes, including photoreceptor axon guidance. rolled is the Drosophila homolog of MAP kinase and a downstream target of EGFR. MAPK has recently been linked to Netrin-dependent growth cone attraction through the Netrin receptor DCC (Forcet *et al.* 2002).

Finally, another important signaling gene that we identified was *NetrinB*. This is one of two Netrin isoforms in Drosophila that are well known for their role in axon guidance, both in the periphery and in central commissural axons that cross the midline. NetrinB is a secreted molecule that can interact with two receptors: *frazzled*, the Drosophila DCC receptor that exerts attractive cues (Kolodziej *et al.* 1996), and *unc-5*, which can mediate repulsive cues in axon guidance (Keleman and Dickson 2001). Although Drosophila Netrins are widely known to be expressed in midline glial cells and in muscles, NetrinB RNA and protein are also found in a number of ventral-lateral neurons in the Drosophila embryo (Harris *et al.* 1996; Mitchell *et al.* 1996). Therefore, the rescue of the $NSF2^{E/Q}$ overgrowth phenotype by presynaptic expression of NetrinB may reveal an autocrine component to this signaling pathway whereby Netrin is released from the growth cone or mature nerve terminal and acts upon Netrin receptors there.

Other notable GS lines recovered: We recovered two other interesting lines that do not fit into the above classifications. First, GS3062 is positioned 0.4 kb upstream of *polo*, which acts as a serine/threonine kinase and hypomorphic alleles of this gene affect larval brain development through cytokinesis defects. However, this GS element is also 3.5 kb upstream of the *soluble NSF attachment protein* (*snap*) gene. The SNAP protein is the cofactor that links NSF to the SNARE complex (Weidman *et al.* 1989; Whiteheart *et al.* 1992) and to AMPA-type glutamate receptors (Osten *et al.* 1998; Hanley *et al.* 2002). Therefore, while *snap* is a very attractive candidate, it remains to be determined whether GS3062

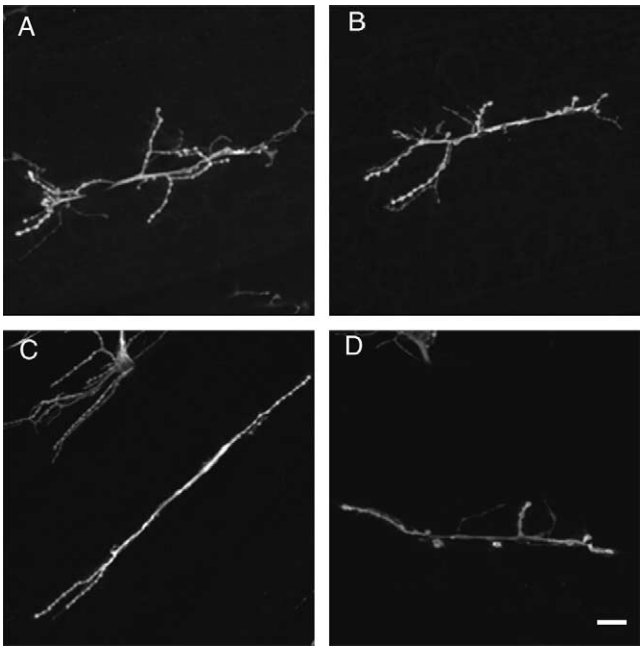

FIGURE 5.—Confirmation of rescue by EP lines. To confirm some of the results from our screen of GS lines, we obtained independently derived EP lines and tested their ability to rescue the *UAS-NSF2*$^{E/Q}$ phenotype. The figure shows NMJs observed in larvae derived from crossing *elav-Gal4*: *UAS-NSF2*$^{E/Q}$ to the following EP lines: (A) *moe[EP1652]*, (B) *nej[EP950]*, (C) *C3G[EP1613]*, and (D) *RhoBTB[EP3099]*.

drives expression of *polo, snap*, or both (see *Confirmation of screen results* below).

Second, we identified GS8030 as a line with the potential to activate *Rab5* expression. This gene is a member of the Rab small GTPase family, and Rab5 in particular is thought to be an important component in the endocytic pathway. Recently, Rab5 has also been shown to be critical for receptor tyrosine-kinase-induced actin remodeling in mouse fibroblasts (LANZETTI *et al.* 2004) and thus there is a potentially interesting link between this gene and the cytoskeleton.

Confirmation of screen results: Since we identified a large number of genes, we sought to generate proof in principle that the GS lines regulate the genes that we identified in Table 1. To this end we used two strategies. First, from the genes listed in Table 1 we identified EP insertions from the Rorth EP collection (RORTH 1996) that regulate some of the genes that we identified in our screen. We obtained the EP lines from the Bloomington Stock Center and tested them for their ability to rescue the *NSF2*$^{E/Q}$ phenotype. Indeed, we found that each showed rescue (Figure 5). Specifically, the lines that we tested were *moe[EP1652]*, *RhoBTB[EP3099]*, *C3G[EP1613]*, and *nej[EP950]*. Since these EP inserts were previously characterized, independently derived unidirectional elements, our finding that each of them rescues the *NSF2*$^{E/Q}$ phenotype greatly strengthens our confidence in the gene identification results shown in Table 1.

Our second approach was to use RT-PCR to determine if one or multiple transcripts are controlled by the GS lines. We therefore designed primers that could be used in quantitative RT-PCR (qRT-PCR) reactions to analyze genes with the potential to be regulated by bidirectional GS lines. For these experiments we used a heat shock-Gal4 driver (hs-Gal4) crossed to the GS line and compared expression levels in hs-Gal4 × GS larvae to the GS larvae alone. In one example, we analyzed transcripts driven by GS2150. This is a bidirectional line that gave strong phenotypic rescue; it is inserted in the 5′-end of *Gli* and also has the potential to upregulate *CG3793*. However, our RT-PCR result clearly shows that the expression of *Gli* is 13-fold higher than that of *CG3793* following heat shock-Gal4 induction 9 (Figure 6). These data clearly indicate that the phenotypic rescue by GS2150 is most likely due to upregulation of *Gli*.

Finally, we were interested in studying GS3062 in more detail. This line carries a bidirectional GS insertion upstream of *polo*, *CG32225*, and nearby S*nap* (Figure 6). We were particularly interested in this region because of the known role of SNAP in mediating interactions between NSF and other proteins, notably the SNARE complex. To study GS3062 further, we used three techniques: first, we carried out RT-PCR to determine which of these nearby genes is upregulated by GS3062; second, we tested unidirectional GS insertions upstream of only *polo* or *Snap* that were not part of our original screen; and third, we tested a *UAS-Snap* transgene, kindly supplied by L. Pallanck (University of Washington).

Our RT-PCR results show that GS3062 increases the expression of *polo* and *CG32225* but not *Snap* (Figure 6), indicating that the ability of GS3062 to rescue the *NSF2*$^{E/Q}$ phenotype is not through *Snap*. To distinguish between the rescuing ability of *polo* and *CG32225*, we next tested the ability of the unidirectional line GS16634, inserted upstream of *polo*, to restore synaptic morphology in *NSF2*$^{E/Q}$ larvae. As shown in Figure 7, GS16634 returns NMJ morphology toward normal, confirming that *polo* is a gene that can rescue the *NSF2*$^{E/Q}$ phenotype. From these data we conclude that upregulation of *polo* by GS3062 leads to restoration of the *NSF2*$^{E/Q}$ phenotype.

In parallel experiments, we independently tested the ability of *Snap* to rescue NMJ overgrowth using GS21416, a unidirectional GS insertion upstream of *Snap* (Figure 6), and a *UAS-Snap* transgene. Serendipitously, both tests showed that upregulation of *Snap* can rescue the *NSF2*$^{E/Q}$ phenotype (Figure 7). This result indicates that a known NSF-interacting protein can restore the mutant phenotype, further strengthening our confidence in our screen.

Therefore, the above data indicate that further delineation of the genes regulated by the GS lines recovered in our screen will be straightforward and that S*nap* is an additional gene that can restore the *NSF2*$^{E/Q}$ phenotype.

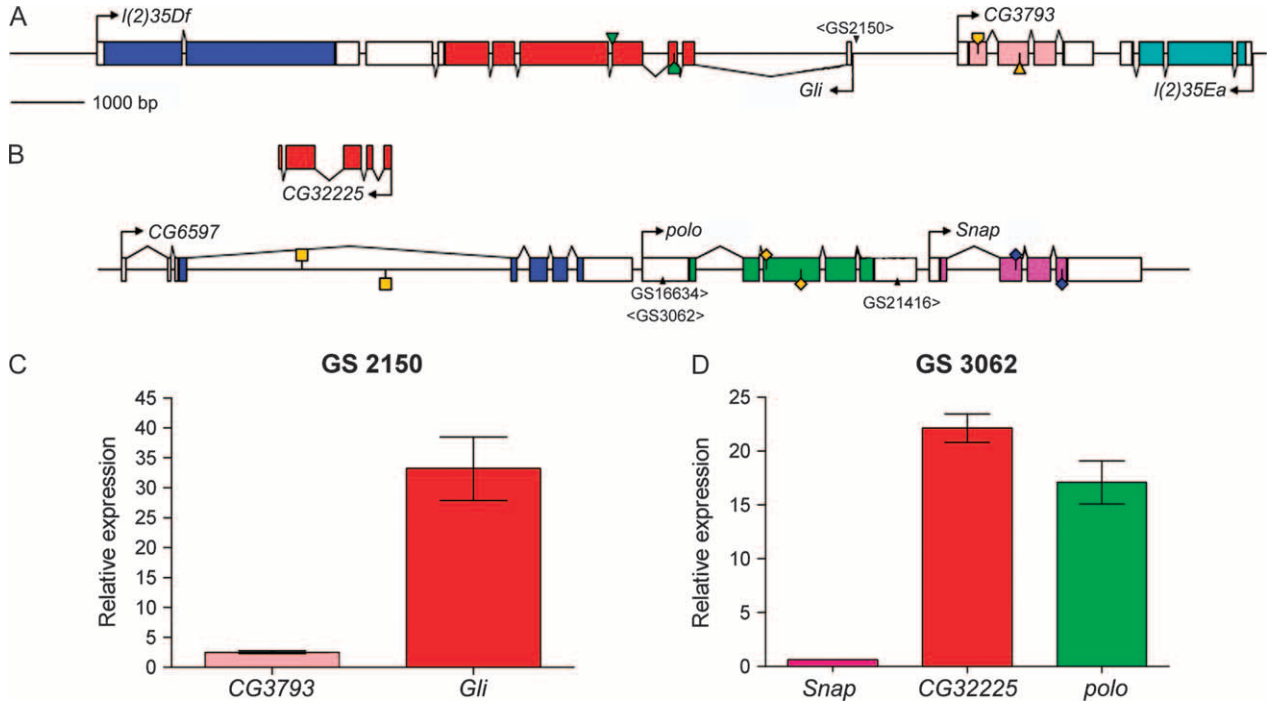

FIGURE 6.—RT-PCR analysis of gene expression in GS2150 and GS3026. To determine which genes are regulated by the bidirectional GS elements identified in our screen, we used RT-PCR. (A and B) The genomic regions surrounding insertions GS2150 and GS3026, respectively. PCR primers locations are indicated by yellow squares for *CG3225*; by yellow diamonds for *polo*; by blue diamonds for *snap*; by a yellow triangle for *CG3793*; and by green triangles for *Gli*. The insertion sites for GS3026, GS16634, GS21416, and GS2150 are also shown. "< >" indicates a bidirectional GS insertion; ">" represents a unidirectional GS insertion, indicating its orientation. Bar in A applies to B as well. (C) qRT-PCR results show an upregulation of *Gli* but not of *CG3793* by GS2150. The bars represent the amount cDNA induced by Gal4 compared to uninduced samples. (D) GS3026 increases expression of both *polo* and *CG32225*. The bar graphs represent the mean and standard error of cDNA levels in four repetitions of hs-Gal4 × GS line larval extracts relative to GS line alone.

Conclusions: Genetic modifier screens have been successfully used to identify genes involved in specific biological processes. For many years such screens were designed as loss-of-function screens for enhancers or suppressors of a given phenotype. More recently, development of Drosophila technology that allows for systematic gain-of-function genetics, namely the EP and Gene Search collections (RORTH 1996; TOBA *et al.* 1999), has allowed screens to identify gain-of-function phenotypes in the wild-type background and also has allowed for modifiers of phenotypes in mutant backgrounds. This gain-of-function analysis is a useful addition to the repertoire of Drosophila genetic techniques because many genes display no loss-of-function phenotype, likely due to functional redundancy among related genes. Thus, increasing gene expression may uncover interacting genes that could not be discovered by loss-of-function analysis.

We have a high degree of confidence in the outcome of our screen. First, all 97 GS lines reported here were screened twice and 74 of the 97 GS lines were screened three times. The 74 lines each showed some degree of rescue on the third pass so we believe that all 97 represent genuine genetic interaction. Second, a number of the genes associated with the GS inserts have been isolated in other neural development screens (ABDELILAH-SEYFRIED *et al.* 2000; KRAUT *et al.* 2001; NORGA *et al.* 2003) and we were thus reassured by having some overlap with previous screens. For example, KRAUT *et al.* (2001) performed a similar screen to the one that we did, except that they screened the EP collection for effects on axon guidance and synaptogenesis in a wild-type background. They reported that, of 2293 EP lines examined, they recorded phenotypes in 114 EPs representing 76 genes. The overlapping genes found in their screen and ours include *amn, Gli*, *LanA*, and *spi*. Finally, we confirmed rescue of the $NSF2^{E/Q}$ phenotype by the GS lines with independently derived lines from the Rorth EP collection of unidirectional UAS driver lines.

While the present screen was efficient at identifying suppressors of the $NSF2^{E/Q}$ overgrowth phenotype, its design places some limitations, common to all gain-of-function screens, on our ability to interpret the outcome. One cautionary possibility is that the GS element causes misexpression of a gene in a tissue where it is not normally found. This is particularly relevant for predicted genes for which there is no prior expression or mutant data. In such cases, we cannot conclude that a particular gene is involved in the $NSF2^{E/Q}$ phenotype. However, finding a misexpression phenotype may indi-

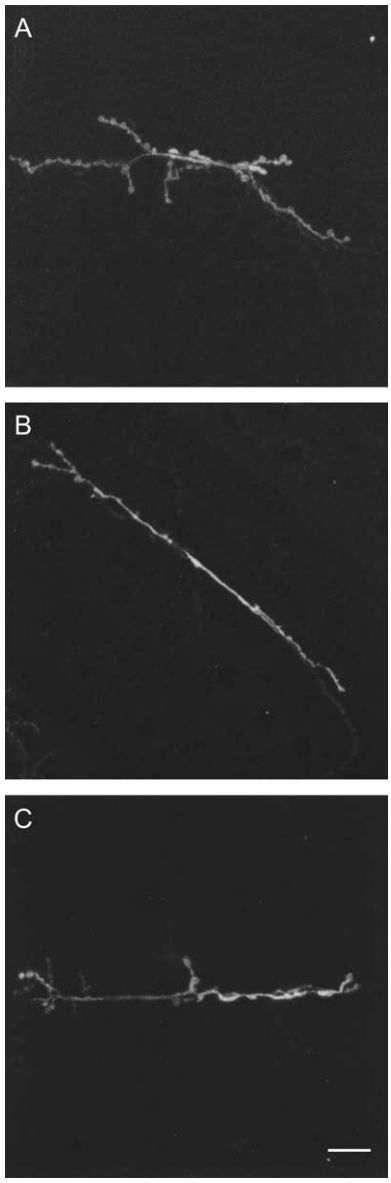

FIGURE 7.—Rescue of *NSF2*$^{E/Q}$ phenotype by *polo* and *Snap*. While investigating GS3062 we also tested the ability of GS16634, GS21416, and *UAS-Snap* to rescue the *NSF2*$^{E/Q}$ phenotype. The insertion positions for GS16634 and GS21416 are shown in Figure 6. (A) A rescued NMJ from an *elav-Gal4*: *UAS-NSF2*$^{E/Q}$*/GS21416* larvae. (B) A rescued NMJ from an *elav-Gal4*: *UAS-NSF2*$^{E/Q}$*/GS21416* larvae. (C) A rescued NMJ from *UAS-Snap/+ ; elav-Gal4*: *UAS-NSF2*$^{E/Q}$/+ larvae. Bar, 25 μm for A–C.

cate the role of a related gene; since the present study was a suppressor screen, such results may be a guide to what type of gene needs to be upregulated to rescue the *NSF2*$^{E/Q}$ phenotype. A second caution is that since some of the GS elements contain two UAS sequences oriented in opposite directions; it is not always straightforward to determine which of the nearby genes may be affected. Finally, if a GS element is inserted near the 3′-end of a gene, but in reverse orientation, there is the possibility of driving expression of an antisense transcript of the upstream gene (RORTH *et al.* 1998). We noted this possibility for 14 of the genes in Table 1.

The NMJ overgrowth phenotype induced by *NSF2*$^{E/Q}$ is a novel one for this molecule (STEWART *et al.* 2002). NSF is well known for its biochemical role in the SNARE cycle, and its role in synaptic vesicle exocytosis has been the subject of intense molecular, genetic, and physiological analysis (WHITEHEART *et al.* 2001), including the study of the *Drosophila comatose* alleles of NSF1 (KAWASAKI *et al.* 1998; TOLAR and PALLANCK 1998). Neural expression of *UAS- NSF2*$^{E/Q}$ induces physiological effects at the NMJ that might be predicted from the known biochemistry of the molecule, but the NMJ developmental effect was unexpected. Indeed, hypomorphic mutants of *n-synaptobrevin* and s*yntaxin* that severely impair transmitter release do not lead to any morphological changes (STEWART *et al.* 2000), signifying that the overgrowth phenotype is unique to NSF and not likely a response to impaired synaptic physiology.

In light of the present findings that components of the cytoskeleton have the potential to reverse the *NSF2*$^{E/Q}$ phenotype, it is noteworthy that substantial proportions of NSF exist in noncytosolic intracellular compartments (MOHTASHAMI *et al.* 2001; PHILLIPS *et al.* 2001). Subcellular fractionation studies of Drosophila NSF1, for example, show that nearly as much NSF1 is found in Triton X-100 insoluble fractions as is found in the cytosolic fractions prepared from normal adult fly heads (MOHTASHAMI *et al.* 2001). The present findings that the *NSF2*$^{E/Q}$ phenotype is rescued by expression of cytoskeletal components, together with those of PHILLIPS *et al.* (2001) who found that both NSF and actin, along with many other proteins, is associated with the presynaptic particle isolated from rat synaptosomes, suggests that this noncytosolic NSF may indeed have a functional role.

It is also remarkable to note that we identified two genes whose products are secreted, *amn* and *NetB*, and another gene, *fz4*, that acts as a receptor for a secreted molecule. These findings may indicate that autocrine signaling is an important component of NMJ development. An interesting linkage can be made between *NetB* and the ubiquitin pathway genes found in this study because CAMPBELL and HOLT (2001) have shown that Netrin activity increases the amount of ubiquinated proteins in the growth cone. Since our ubiquitin results all indicate a need for increased ubiquitin pathway function to rescue *NSF2*$^{E/Q}$, the secretion and autocrine action of NetrinB may also positively regulate the ubiquitin pathway.

Our goal here was to identify potential genetic interactions with NSF. Further studies that examine loss-of-function phenotypes, gene expression, and protein localization of the candidate genes are required to further our goal. These data represent a substantial resource that will aid our efforts to understand the role

of NSF in neuromuscular junction development and point to novel functions of NSF.

We thank Corey Goodman for the Sh-GFP-CD8 stock, Jammie Tosevski for help setting up crosses in the initial screen, and Neha Sharma, Manpreet Kaur, Joseph Barbero, and Sara Seabrooke for help maintaining fly stocks. This work was financially supported by grants from The Natural Sciences and Engineering Research Council of Canada, the Canada Foundation for Innovation, the Ontario Innovation Trust, and the Canada Research Chairs Program to B.A.S. and from the Ministry of Education, Culture, Sports, Science and Technology of Japan (no. 12202002) to T.A. B.A.S. is a member of the Canada Foundation for Innovation Centre for the Neurobiology of Stress and the Integrative Behavior and Neuroscience Group at the University of Toronto at Scarborough.

LITERATURE CITED

Abdelilah-Seyfried, S., Y. M. Chan, C. Zeng, N. J. Justice, S. Younger-Shepherd *et al.*, 2000 A gain-of-function screen for genes that affect the development of the Drosophila adult external sensory organ. Genetics **155:** 733–752.

Block, M. R., B. S. Glick, C. A. Wilcox, F. T. Wieland and J. E. Rothman, 1988 Purification of an N-ethylmaleimide-sensitive protein catalyzing vesicular transport. Proc. Natl. Acad. Sci. USA **85:** 7852–7856.

Boulianne, G. L., and W. S. Trimble, 1995 Identification of a second homolog of N-ethylmaleimide-sensitive fusion protein that is expressed in the nervous system and secretory tissues of Drosophila. Proc. Natl. Acad. Sci. USA **92:** 7095–7099.

Campbell, D. S., and C. E. Holt, 2001 Chemotropic responses of retinal growth cones mediated by rapid local protein synthesis and degradation. Neuron **32:** 1013–1026.

Cong, M., S. J. Perry, L. A. Hu, P. I. Hanson, A. Claing *et al.*, 2001 Binding of the beta2 adrenergic receptor to N-ethylmaleimide-sensitive factor regulates receptor recycling. J. Biol. Chem. **276:** 45145–45152.

Delon, I., H. Chanut-Delalande and F. Payre, 2003 The Ovo/Shavenbaby transcription factor specifies actin remodelling during epidermal differentiation in Drosophila. Mech. Dev. **120:** 747–758.

Diantonio, A., A. P. Haghighi, S. L. Portman, J. D. Lee, A. M. Amaranto *et al.*, 2001 Ubiquitination-dependent mechanisms regulate synaptic growth and function. Nature **412:** 449–452.

Eby, J. J., S. P. Holly, F. Van Drogen, A. V. Grishin, M. Peter *et al.*, 1998 Actin cytoskeleton organization regulated by the PAK family of protein kinases. Curr. Biol. **8:** 967–970.

Forcet, C., E. Stein, L. Pays, V. Corset, F. Llambi *et al.*, 2002 Netrin-1-mediated axon outgrowth requires deleted in colorectal cancer-dependent MAPK activation. Nature **417:** 443–447.

Fyrberg, E. A., J. W. Mahaffey, B. J. Bond and N. Davidson, 1983 Transcripts of the six Drosophila actin genes accumulate in a stage- and tissue-specific manner. Cell **33:** 115–123.

Golby, J. A., L. A. Tolar and L. Pallanck, 2001 Partitioning of *N*-ethylmaleimide-sensitive fusion (NSF) protein function in *Drosophila melanogaster*: dNSF1 is required in the nervous system, and dNSF2 is required in mesoderm. Genetics **158:** 265–278.

Han, S. Y., D. Y. Park, S. D. Park and S. H. Hong, 2000 Identification of Rab6 as an N-ethylmaleimide-sensitive fusion protein-binding protein. Biochem. J. **352** (Pt. 1): 165–173.

Hanley, J. G., L. Khatri, P. I. Hanson and E. B. Ziff, 2002 NSF ATPase and alpha-/beta-SNAPs disassemble the AMPA receptor-PICK1 complex. Neuron **34:** 53–67.

Harris, R., L. M. Sabatelli and M. A. Seeger, 1996 Guidance cues at the Drosophila CNS midline: identification and characterization of two Drosophila Netrin/UNC-6 homologs. Neuron **17:** 217–228.

Hooper, J. E., 1994 Distinct pathways for autocrine and paracrine Wingless signalling in Drosophila embryos. Nature **372:** 461–464.

Huang, Y., R. T. Baker and J. A. Fischer-Vize, 1995 Control of cell fate by a deubiquitinating enzyme encoded by the fat facets gene. Science **270:** 1828–1831.

Ishimaru, S., R. Williams, E. Clark, H. Hanafusa and U. Gaul, 1999 Activation of the Drosophila C3G leads to cell fate changes and overproliferation during development, mediated by the RAS-MAPK pathway and RAP1. EMBO J. **18:** 145–155.

Janson, K., E. D. Cohen and E. L. Wilder, 2001 Expression of DWnt6, DWnt10, and DFz4 during Drosophila development. Mech. Dev. **103:** 117–120.

Karagiosis, S. A., and D. F. Ready, 2004 Moesin contributes an essential structural role in Drosophila photoreceptor morphogenesis. Development **131:** 725–732.

Karim, F. D., and G. M. Rubin, 1999 PTP-ER, a novel tyrosine phosphatase, functions downstream of Ras1 to downregulate MAP kinase during Drosophila eye development. Mol. Cell **3:** 741–750.

Kawasaki, F., A. M. Mattiuz and R. W. Ordway, 1998 Synaptic physiology and ultrastructure in comatose mutants define an in vivo role for NSF in neurotransmitter release. J. Neurosci. **18:** 10241–10249.

Keleman, K., and B. J. Dickson, 2001 Short- and long-range repulsion by the Drosophila Unc5 netrin receptor. Neuron **32:** 605–617.

Kiehart, D. P., C. G. Galbraith, K. A. Edwards, W. L. Rickoll and R. A. Montague, 2000 Multiple forces contribute to cell sheet morphogenesis for dorsal closure in Drosophila. J. Cell Biol. **149:** 471–490.

Kolodziej, P. A., L. C. Timpe, K. J. Mitchell, S. R. Fried, C. S. Goodman *et al.*, 1996 frazzled encodes a Drosophila member of the DCC immunoglobulin subfamily and is required for CNS and motor axon guidance. Cell **87:** 197–204.

Kraut, R., K. Menon and K. Zinn, 2001 A gain-of-function screen for genes controlling motor axon guidance and synaptogenesis in Drosophila. Curr. Biol. **11:** 417–430.

Lanzetti, L., A. Palamidessi, L. Areces, G. Scita and P. P. Di Fiore, 2004 Rab5 is a signalling GTPase involved in actin remodelling by receptor tyrosine kinases. Nature **429:** 309–314.

Lin, Y. J., L. Seroude and S. Benzer, 1998 Extended life-span and stress resistance in the Drosophila mutant methuselah. Science **282:** 943–946.

Marek, K. W., R. Fetter, S. Smolik, C. S. Goodman and G. W. Davis, 2000 A genetic analysis of synaptic development: pre- and postsynaptic dCBP control transmitter release at the Drosophila NMJ. Neuron **25:** 537–547.

McDonald, P. H., N. L. Cote, F. T. Lin, R. T. Premont, J. A. Pitcher *et al.*, 1999 Identification of NSF as a beta-arrestin1-binding protein. Implications for beta2-adrenergic receptor regulation. J. Biol. Chem. **274:** 10677–10680.

Mitchell, K. J., J. L. Doyle, T. Serafini, T. E. Kennedy, M. Tessier-Lavigne *et al.*, 1996 Genetic analysis of Netrin genes in Drosophila: Netrins guide CNS commissural axons and peripheral motor axons. Neuron **17:** 203–215.

Mohtashami, M., B. A. Stewart, G. L. Boulianne and W. S. Trimble, 2001 Analysis of the mutant Drosophila N-ethylmaleimide sensitive fusion-1 protein in comatose reveals molecular correlates of the behavioural paralysis. J. Neurochem. **77:** 1407–1417.

Muller, J. M., J. Shorter, R. Newman, K. Deinhardt, Y. Sagiv *et al.*, 2002 Sequential SNARE disassembly and GATE-16-GOS-28 complex assembly mediated by distinct NSF activities drives Golgi membrane fusion. J. Cell Biol. **157:** 1161–1173.

Muralidhar, M. G., and J. B. Thomas, 1993 The Drosophila bendless gene encodes a neural protein related to ubiquitin-conjugating enzymes. Neuron **11:** 253–266.

Nishimune, A., J. T. Isaac, E. Molnar, J. Noel, S. R. Nash *et al.*, 1998 NSF binding to GluR2 regulates synaptic transmission. Neuron **21:** 87–97.

Noel, J., G. S. Ralph, L. Pickard, J. Williams, E. Molnar *et al.*, 1999 Surface expression of AMPA receptors in hippocampal neurons is regulated by an NSF-dependent mechanism. Neuron **23:** 365–376.

Noguchi, T., and K. G. Miller, 2003 A role for actin dynamics in individualization during spermatogenesis in Drosophila melanogaster. Development **130:** 1805–1816.

Norga, K. K., M. C. Gurganus, C. L. Dilda, A. Yamamoto, R. F. Lyman *et al.*, 2003 Quantitative analysis of bristle number in Drosophila mutants identifies genes involved in neural development. Curr. Biol. **13:** 1388–1396.

Oh, C. E., R. McMahon, S. Benzer and M. A. Tanouye, 1994 bendless, a Drosophila gene affecting neuronal connectivity, encodes

a ubiquitin-conjugating enzyme homolog. J. Neurosci. **14:** 3166–3179.

Osten, P., S. Srivastava, G. J. Inman, F. S. Vilim, L. Khatri *et al.*, 1998 The AMPA receptor GluR2 C terminus can mediate a reversible, ATP-dependent interaction with NSF and alpha- and beta-SNAPs. Neuron **21:** 99–110.

Packard, M., E. S. Koo, M. Gorczyca, J. Sharpe, S. Cumberledge *et al.*, 2002 The Drosophila Wnt, wingless, provides an essential signal for pre- and postsynaptic differentiation. Cell **111:** 319–330.

Paglini, G., P. Kunda, S. Quiroga, K. Kosik and A. Caceres, 1998 Suppression of radixin and moesin alters growth cone morphology, motility, and process formation in primary cultured neurons. J. Cell Biol. **143:** 443–455.

Pallanck, L., R. W. Ordway, M. Ramaswami, W. Y. Chi, K. S. Krishnan *et al.*, 1995 Distinct roles for N-ethylmaleimide-sensitive fusion protein (NSF) suggested by the identification of a second Drosophila NSF homolog. J. Biol. Chem. **270:** 18742–18744.

Parlati, F., T. Weber, J. A. McNew, B. Westermann, T. H. Sollner *et al.*, 1999 Rapid and efficient fusion of phospholipid vesicles by the alpha-helical core of a SNARE complex in the absence of an N-terminal regulatory domain. Proc. Natl. Acad. Sci. USA **96:** 12565–12570.

Parnas, D., A. P. Haghighi, R. D. Fetter, S. W. Kim and C. S. Goodman, 2001 Regulation of postsynaptic structure and protein localization by the Rho-type guanine nucleotide exchange factor dPix. Neuron **32:** 415–424.

Phillips, G. R., J. K. Huang, Y. Wang, H. Tanaka, L. Shapiro *et al.*, 2001 The presynaptic particle web: ultrastructure, composition, dissolution, and reconstitution. Neuron **32:** 63–77.

Prokopenko, S. N., Y. He, Y. Lu and H. J. Bellen, 2000 Mutations affecting the development of the peripheral nervous system in Drosophila: a molecular screen for novel proteins. Genetics **156:** 1691–1715.

Ratti, A., F. Amati, M. Bozzali, E. Conti, F. Sangiuolo *et al.*, 2001 Cloning and molecular characterization of three ubiquitin fusion degradation 1 (Ufd1) ortholog genes from Xenopus laevis, Gallus gallus and Drosophila melanogaster. Cytogenet. Cell Genet. **92:** 279–282.

Rorth, P., 1996 A modular misexpression screen in Drosophila detecting tissue-specific phenotypes. Proc. Natl. Acad. Sci. USA **93:** 12418–12422.

Rorth, P., K. Szabo, A. Bailey, T. Laverty, J. Rehm *et al.*, 1998 Systematic gain-of-function genetics in Drosophila. Development **125:** 1049–1057.

Salzberg, A., S. N. Prokopenko, Y. He, P. Tsai, M. Pal *et al.*, 1997 *P*-element insertion alleles of essential genes on the third chromosome of *Drosophila melanogaster*: mutations affecting embryonic PNS development. Genetics **147:** 1723–1741.

Sepp, K. J., and V. J. Auld, 2003 RhoA and Rac1 GTPases mediate the dynamic rearrangement of actin in peripheral glia. Development **130:** 1825–1835.

Sollner, T., M. K. Bennett, S. W. Whiteheart, R. H. Scheller and J. E. Rothman, 1993a A protein assembly-disassembly pathway in vitro that may correspond to sequential steps of synaptic vesicle docking, activation, and fusion. Cell **75:** 409–418.

Sollner, T., S. W. Whiteheart, M. Brunner, H. Erdjument-Bromage, S. Geromanos *et al.*, 1993b SNAP receptors implicated in vesicle targeting and fusion. Nature **362:** 318–324.

Song, I., S. Kamboj, J. Xia, H. Dong, D. Liao *et al.*, 1998 Interaction of the N-ethylmaleimide-sensitive factor with AMPA receptors. Neuron **21:** 393–400.

Song, W., R. Ranjan, K. Dawson-Scully, P. Bronk, L. Marin *et al.*, 2002 Presynaptic regulation of neurotransmission in Drosophila by the g protein-coupled receptor methuselah. Neuron **36:** 105–119.

Stewart, B. A., H. L. Atwood, J. J. Renger, J. Wang and C. F. Wu, 1994 Improved stability of Drosophila larval neuromuscular preparations in haemolymph-like physiological solutions. J. Comp. Physiol. A **175:** 179–191.

Stewart, B. A., M. Mohtashami, W. S. Trimble and G. L. Boulianne, 2000 SNARE proteins contribute to calcium cooperativity of synaptic transmission. Proc. Natl. Acad. Sci. USA **97:** 13955–13960.

Stewart, B. A., M. Mohtashami, L. Zhou, W. S. Trimble and G. L. Boulianne, 2001 SNARE-dependent signaling at the Drosophila wing margin. Dev. Biol. **234:** 13–23.

Stewart, B. A., M. Mohtashami, P. Rivlin, D. L. Deitcher, W. S. Trimble *et al.*, 2002 Dominant-negative NSF2 disrupts the structure and function of Drosophila neuromuscular synapses. J. Neurobiol. **51:** 261–271.

Toba, G., T. Ohsako, N. Miyata, T. Ohtsuka, K. H. Seong *et al.*, 1999 The gene search system: a method for efficient detection and rapid molecular identification of genes in *Drosophila melanogaster*. Genetics **151:** 725–737.

Tolar, L. A., and L. Pallanck, 1998 NSF function in neurotransmitter release involves rearrangement of the SNARE complex downstream of synaptic vesicle docking. J. Neurosci. **18:** 10250–10256.

Vernooy, S. Y., V. Chow, J. Su, K. Verbrugghe, J. Yang *et al.*, 2002 Drosophila Bruce can potently suppress Rpr- and Grim-dependent but not Hid-dependent cell death. Curr. Biol. **12:** 1164–1168.

Wan, H. I., A. Diantonio, R. D. Fetter, K. Bergstrom, R. Strauss *et al.*, 2000 Highwire regulates synaptic growth in Drosophila. Neuron **26:** 313–329.

Weber, T., B. V. Zemelman, J. A. McNew, B. Westermann, M. Gmachl *et al.*, 1998 SNAREpins: minimal machinery for membrane fusion. Cell **92:** 759–772.

Weidman, P. J., P. Melancon, M. R. Block and J. E. Rothman, 1989 Binding of an N-ethylmaleimide-sensitive fusion protein to Golgi membranes requires both a soluble protein(s) and an integral membrane receptor. J. Cell Biol. **108:** 1589–1596.

Whiteheart, S. W., and E. A. Matveeva, 2004 Multiple binding proteins suggest diverse functions for the N-ethylmaleimide sensitive factor. J. Struct. Biol. **146:** 32–43.

Whiteheart, S. W., M. Brunner, D. W. Wilson, M. Wiedmann and J. E. Rothman, 1992 Soluble N-ethylmaleimide-sensitive fusion attachment proteins (SNAPs) bind to a multi-SNAP receptor complex in Golgi membranes. J. Biol. Chem. **267:** 12239–12243.

Whiteheart, S. W., K. Rossnagel, S. A. Buhrow, M. Brunner, R. Jaenicke *et al.*, 1994 N-ethylmaleimide-sensitive fusion protein: a trimeric ATPase whose hydrolysis of ATP is required for membrane fusion. J. Cell Biol. **126:** 945–954.

Whiteheart, S. W., T. Schraw and E. A. Matveeva, 2001 N-ethylmaleimide sensitive factor (NSF) structure and function. Int. Rev. Cytol. **207:** 71–112.

Wilson, R., L. Goyal, M. Ditzel, A. Zachariou, D. A. Baker *et al.*, 2002 The DIAP1 RING finger mediates ubiquitination of Dronc and is indispensable for regulating apoptosis. Nat. Cell Biol. **4:** 445–450.

Xu, Z., K. Sato and W. Wickner, 1998 LMA1 binds to vacuoles at Sec18p (NSF), transfers upon ATP hydrolysis to a t-SNARE (Vam3p) complex, and is released during fusion. Cell **93:** 1125–1134.

Zhong, Y., V. Budnik and C. F. Wu, 1992 Synaptic plasticity in Drosophila memory and hyperexcitable mutants: role of cAMP cascade. J. Neurosci. **12:** 644–651.

Zito, K., R. D. Fetter, C. S. Goodman and E. Y. Isacoff, 1997 Synaptic clustering of Fascilin II and Shaker: essential targeting sequences and role of Dlg. Neuron **19:** 1007–1016.

Zito, K., D. Parnas, R. D. Fetter, E. Y. Isacoff and C. S. Goodman, 1999 Watching a synapse grow: noninvasive confocal imaging of synaptic growth in Drosophila. Neuron **22:** 719–729.

Communicating editor: R. S. Hawley